

membranes formed by self-assembly<sup>26</sup>. The elastic constants and the diffraction peak profiles of single domains of this new phase should be carefully examined and compared to these predictions.

From the point of view of materials chemistry, the approach described here should lead to the discovery of a whole new class of mineral lamellar liquid crystalline phases. Indeed, from current work, we expect that similar phase behaviour will be found not only in other related members of the series  $H_3M_3Z_2O_{14}$  (with for example  $M = Sb, Nb, Ta; Z = P, As$ ), but also in phases such as  $HM_2Nb_3O_{10}$  ( $M = Pb, Ca$ ),  $HTiNbO_5$  or  $Zr(HPO_4)_2 \cdot H_2O$  that can all be fully exfoliated using tetra(*n*-butyl)ammonium hydroxide<sup>27,28</sup>. All of these phases, because of the robustness of their layers, could be used for polymerization of soluble species under tunable two-dimensional confinement conditions. □

Received 8 January; accepted 25 July 2001.

- Eigler, D. M. & Schweizer, E. K. Positioning single atoms with a scanning tunneling microscope. *Nature* **344**, 524–526 (1990).
- Poncharal, P., Wang, Z. L., Ugarte, D. & de Heer, W. A. Electrostatic deflections and electromechanical resonances of carbon nanotubes. *Science* **283**, 1513–1516 (1999).
- Blanco, A. *et al.* Large-scale synthesis of a silicon photonic crystal with a complete three-dimensional bandgap near 1.5 micrometres. *Nature* **405**, 437–440 (2000).
- Davidson, P., Gabriel, J.-C., Levelut, A.-M. & Batail, P. Nematic liquid crystalline mineral polymers. *Adv. Mater.* **5**, 665–668 (1993).
- Gabriel, J.-C. P. & Davidson, P. New trends in colloidal liquid crystals based on mineral moieties. *Adv. Mater.* **12**, 9–20 (2000).
- Kajiwara, K., Donkai, N., Hiragi, Y. & Inagaki, H. Lyotropic mesophase of imogolite 1. Effect of polydispersity on phase diagram. *Makromol. Chem.* **187**, 2883–2894 (1986).
- Nikobakht, B., Wang, Z. L. & El-Sayed, M. A. Self-assembly of gold nanorods. *J. Phys. Chem. B* **104**, 1346–1348 (2000).
- Maeda, Y. & Hachisu, S. Schiller layers in beta-ferric oxyhydroxide sol as an order–disorder phase separating system. *Coll. Surf.* **6**, 1–16 (1983).
- Brown, A. B. D., Ferrero, C., Narayanan, T. & Rennie, A. R. Phase separation and structure in a concentrated colloidal dispersion of uniform plates. *Eur. Phys. J. B* **11**, 481–489 (1999).
- van der Kooij, F. M., Kassapidou, K. & Lekkerkerker, H. N. W. Liquid crystal phase transitions in suspensions of polydisperse plate-like particles. *Nature* **406**, 868–871 (2000).
- Fraden, S. in *Observation, Prediction, and Simulation of Phase Transitions in Complex Fluids* (eds Baus, M., Rull, L. F. & Ryckaert, J. P.) 113–164 (NATO ASI Series, Kluwer Academic, Dordrecht, 1995).
- Whittingham, M. W. & Jacobson, A. J. *Intercalation Chemistry* (Academic, New York, 1982).
- Gabriel, J.-C. P., Sanchez, C. & Davidson, P. Observation of nematic liquid-crystal textures in aqueous gels of smectite clays. *J. Phys. Chem.* **100**, 11139–11143 (1996).
- Mourchid, A., Lécolier, E., Van Damme, H. & Levitz, P. On viscoelastic, birefringent, and swelling properties of laponite clay suspensions: revisited phase diagram. *Langmuir* **14**, 4718–4723 (1998).
- Piffard, Y., Verbaere, A., Lachgar, A., Deniard-Courant, S. & Tournoux, M. The layered phosphoantimonic acid  $H_3Sb_3P_2O_{14} \cdot xH_2O$ . *Rev. Chim. Miner.* **23**, 766–775 (1986).
- Boesecke, P., Diat, O. & Rasmussen, B. High-brilliance beamline at the European Synchrotron Radiation Facility. *Rev. Sci. Instrum.* **66**, 1636–1638 (1995).
- Safinya, C. R. *et al.* Steric interaction in a model multilayer system: a synchrotron study. *Phys. Rev. Lett.* **57**, 2718–2721 (1986).
- Salditt, T. *et al.* Specular and diffuse scattering of highly aligned phospholipid membranes. *Phys. Rev. E* **60**, 7285–7289 (1999).
- Deryagin, B. V. & Landau, L. Theory of the stability of strongly charged lyophobic sols and of the adhesion of strongly charged particles in solutions of electrolytes. *Acta Physicochim. URSS* **14**, 633–662 (1941).
- Verwey, E. J. W. & Overbeek, J. Th. G. *Theory of the Stability of Lyophobic Colloids* (Elsevier, Amsterdam, 1948).
- Safinya, C. R. *et al.* Structure of membrane surfactant and liquid-crystalline smectic lamellar phases under flow. *Science* **261**, 588–591 (1993).
- Tjandra, N. & Bax, A. Direct measurement of distances and angles in biomolecules by NMR in a dilute liquid crystalline medium. *Science* **278**, 1111–1114 (1997).
- Desvaux, H., Gabriel, J.-C. P., Berthault, P. & Camerel, F. First use of a mineral liquid crystal for NMR measurement of residual dipolar couplings of a non-labeled biomolecule. *Angew. Chem.* **40**, 373–376 (2001).
- Ramirez, B. E. & Bax, A. Modulation of the alignment tensor of macromolecules dissolved in a dilute liquid crystalline medium. *J. Am. Chem. Soc.* **120**, 9106–9107 (1998).
- Janiak, M. J., Small, D. M. & Shipley, G. G. Nature of the thermal pretransition of synthetic phospholipids: Dimyristoyl- and Dipalmitoyllecithin. *Biochemistry* **15**, 4575–4580 (1976).
- Toner, J. New phase of matter in lamellar phases of tethered, crystalline membranes. *Phys. Rev. Lett.* **64**, 1741–1744 (1990).
- Fang, M. *et al.* Layer by layer growth and condensation reactions of niobate and titanoniobate thin films. *Chem. Mater.* **11**, 1526–1532 (1999).
- Kaschak, D. M. *et al.* Chemistry on the edge: a microscopic analysis of the intercalation, exfoliation, edge functionalization and monolayer surface tiling reactions of  $\alpha$ -zirconium phosphate. *J. Am. Chem. Soc.* **120**, 10887–10894 (1998).
- Kay, L. E., Keifer, P. & Saarinen, T. Pure absorption gradient enhanced heteronuclear single quantum correlation spectroscopy with improved sensitivity. *J. Am. Chem. Soc.* **114**, 10663–10665 (1992).

Supplementary information is available on Nature's World-Wide Web site (<http://www.nature.com>) or as paper copy from the London editorial office of Nature.

## Acknowledgements

We thank the LURE and ESRF synchrotron radiation facilities for the award of beamtime, C. Bourgaux, P. Panine and T. Narayanan for technical support at D24 (LURE) and ID2 (ESRF), Y. Piffard for supplying us with 1g of  $H_3Sb_3P_2O_{14}$  powder at the start of this work, C. Chaudemanche and X. Leguevel for their participation in the synthesis of large amounts of  $H_3Sb_3P_2O_{14}$ , F. Alvarez for pH measurements, S. Grolleau for TGA measurements, P. Berthault and D. Jeannerat for their help in NMR measurements and processing of the spectra, P. Sinay and Y. Zhang for the gift of the pentasaccharide and J. P. Simorre for giving us access to a 18.7 T magnet while we were performing our SAXS experiments at the ESRF. Financial support from the Ministry of Education (PhD fellowship for F.C.), the Ecole Normale Supérieure and the Ecole Nationale des Ponts et Chaussées (PhD fellowships for B.L.), the Région Pays de Loire and the GDR-CNRS 690 FORMES (for  $D_2O$ ) is gratefully acknowledged.

Correspondence and requests for materials should be addressed to J.-C.P.G. (e-mail: [jeang@covalentmaterials.com](mailto:jeang@covalentmaterials.com)) or P.D. (e-mail: [davidson@lps.u-psud.fr](mailto:davidson@lps.u-psud.fr)).

## High frequency of 'super-cyclones' along the Great Barrier Reef over the past 5,000 years

Jonathan Nott\* & Matthew Hayne†

\* School of Tropical Environment Studies and Geography, James Cook University, PO Box 6811, Cairns, Queensland, 4870, Australia

† Australian Geological Survey Organisation, GPO Box 378, Canberra, Australian Capital Territory, 2601 Australia

Understanding long-term variability in the occurrence of tropical cyclones that are of extreme intensity is important for determining their role in ecological disturbances<sup>1–5</sup>, for predicting present and future community vulnerability and economic loss<sup>6</sup> and for assessing whether changes in the variability of such cyclones are induced by climate change<sup>7</sup>. Our ability to accurately make these assessments has been limited by the short (less than 100 years) instrumented record of cyclone intensity. Here we determine the intensity of prehistoric tropical cyclones over the past 5,000 years from ridges of detrital coral and shell deposited above highest tide and terraces that have been eroded into coarse-grained alluvial fan deposits. These features occur along 1,500 km of the Great Barrier Reef and also the Gulf of Carpentaria, Australia. We infer that the deposits were formed by storms with recurrence intervals of two to three centuries<sup>8–11</sup>, and we show that the cyclones responsible must have been of extreme intensity (central pressures less than 920 hPa). Our estimate of the frequency of such 'super-cyclones' is an order of magnitude higher than that previously estimated (which was once every several millennia<sup>12–14</sup>), and is sufficiently high to suggest that the character of rainforests and coral reef communities were probably shaped by these events.

In tropical, intraplate settings that are largely free from the effects of sizeable earthquakes, tsunami, volcanic eruptions and landslides, tropical cyclones rank as one of the main hazards affecting both natural and human communities. In natural communities, disturbance by hazards is one of the most important mechanisms affecting the evolution and diversity of species<sup>1–5</sup>. Because of the short timescales over which direct and continuous observation of change within ecological communities is possible<sup>5</sup>, it has been difficult to assess the influence of various scales of disturbance, and whether other mechanisms such as recruitment limitation<sup>15</sup> are

significant. The short length of the instrumented record also presents a similar conundrum for human communities. Next to drought, tropical cyclones have the greatest effect on economies and human life of any natural hazards<sup>16</sup>. The insurance industry relies on models of future economic loss that use records of cyclone activity extending back usually no more than a century and often less than 50 yr—periods too short from which to make reliable predictions. Cyclones have also been predicted to increase in magnitude and possibly frequency under an enhanced greenhouse climate<sup>7,17</sup>, but assessing whether any variation is a function of anthropogenic effects requires decoupling recent and future trends from longer-term periodicities. Millennial-scale records of tropical cyclone frequency have been obtained for many areas of the Great Barrier Reef<sup>8–11</sup> (GBR), but to date there has been no information available on the intensity of these events. With the inclusion of such information it would be possible to accurately assess long-term periodicities and trends in the behaviour of tropical cyclones—particularly those of extreme intensity, referred to here as super-cyclones (extreme category 4 and category 5 storms on the Saffir–Simpson scale).

Storm ridge development occurs when cyclonic waves and surge deposit lithic and biogenic (coral and shell) sediment farther inland than the highest astronomical tide. Most ridges are composed of single storm deposits, which are made up of several facies including storm beach face, berm, crest and washover elements. Beach face and berm facies include porous, clast supported, coarse biogenic shingle deposits that occasionally dip seawards but are usually structureless. Crest facies are horizontally bedded, and are finer-grained than beach-face deposits. Washover facies are bedded, dip landwards up to 15° and sometimes contain imbricated clasts (imbrication is a sedimentary fabric where particles are arranged in an overlapping shingle-like pattern dipping in one direction). Storm deposits are often separated by ‘groundsurfaces’, which are lenses of pumice pebbles and a weak sooty or earthy palaeosol<sup>10,11</sup>. An individual storm deposit is generally thought to represent one storm event, on the basis of sedimentary architecture, groundsurfaces and detailed chronologies. Supporting this assumption are observations of single coral shingle storm

ridges—up to 18 km long, 37 m wide and 3.5 m high—being deposited during individual tropical cyclones<sup>18–21</sup>. The storm deposits analysed in this study occur as multiple, shore-parallel ridges on tectonically stable coasts and islands (Fig. 1a, b). The age of each consecutive deposit/ridge increases progressively with distance from shore (Fig. 1b).

Terraces occur when waves and surge leave erosional scarps. They occur within raised gravel beach deposits, in this instance reworked from coarse-grained alluvial fans. These ridges and terraces are a function of mean storm ‘still’ water level (storm surge, tide and wave set-up) and wave run-up. (Here, ‘surge’ is the rise in water level due to lowered atmospheric pressure and surface wind stress; ‘set-up’ is the rise in water level due to the action of breaking waves; and ‘run-up’ is the rush of water up against a structure or beach.) The frequency and intensity of past cyclones are determined by geologically dating and topographically surveying these features, then running numerical models that estimate surge and wave heights necessary to reach these levels (see Methods).

The ridge sequences used in this analysis occur at Princess Charlotte Bay (PCB) towards the northern end of the GBR, Fitzroy, Normanby and Curacoa islands within the central GBR, and Lady Elliot island in the south. Wallaby island lies in the Gulf of Carpentaria. A sequence of four erosional terraces occur at Red Cliff (Fig. 1a). Radiocarbon dates from these deposits reveal that the storms responsible have a mean return interval of 177 yr at PCB and 280 yr at Curacoa island over the past 5,000 yr (refs 8, 10, 11), 253 yr at Lady Elliot island over the past 3,200 yr (ref. 9), and approximately 180 yr at Wallaby island over the last 4,100 yr (see Methods). The ridges at Fitzroy and Normanby islands and terraces at Red Cliff are fewer in number and formed over the past few hundred years (Table 1).

Our analyses show that most ridges on Fitzroy, Normanby, Curacoa, Lady Elliot and Wallaby islands and the highest terraces at Red Cliff were emplaced during category 5 cyclones, which probably had central pressures of less than 920 hPa (Fig. 2; Table 2). Even at the 95% uncertainty margin, these cyclones were still category 5 or at least severe category 4 events. The storms responsible for construction of the ridges at PCB appear to have

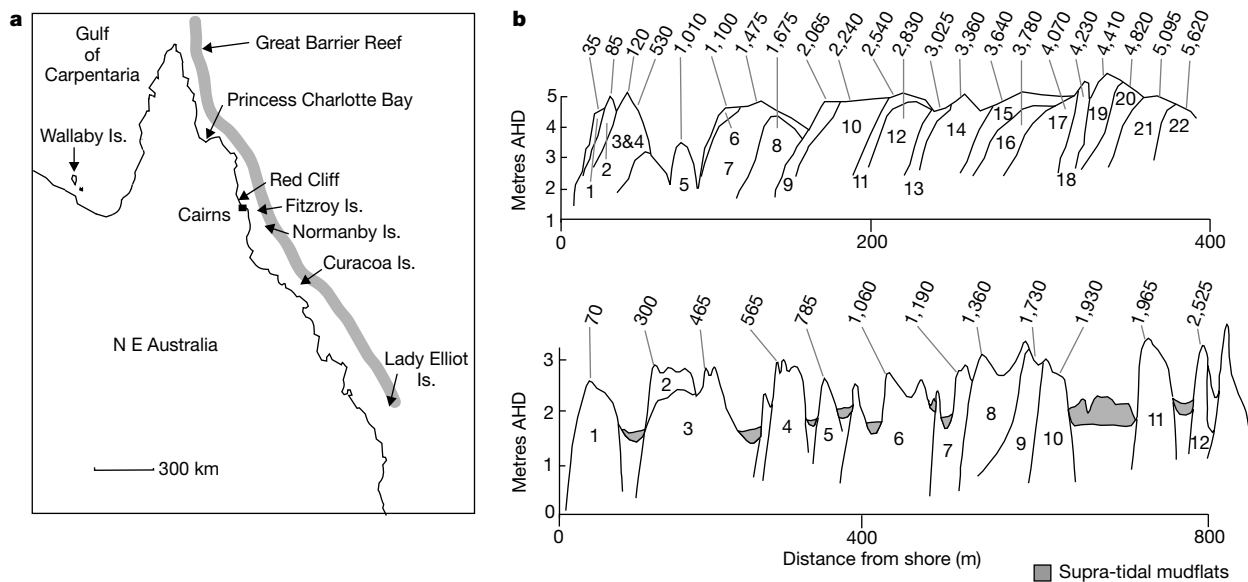


**Figure 1** Study sites and storm deposit data. **a**, Location map of study sites. **b**, Stratigraphic relationship of storm deposit/ridges on Curacoa island (top) and Princess Charlotte Bay (bottom). Successive storm deposits are numbered accordingly. Mean

reservoir-corrected radiocarbon age (in yr BP) for each ridge is shown above traces. Note progressive increase in age with distance inland. Age details in Table 1. Cross-sections modified from refs 10 and 11. AHD is Australian Height Datum.

**Table 1 Radiocarbon ages for coral shingle storm deposits**

Location	Sample code	Radiocarbon age (yr BP)	Calibrated 2σ age (yr BP)
Wallaby 1	ANU 9229	350 ± 80	290–480
Wallaby 3	ANU 9230	570 ± 90	520–650
Wallaby 21	ANU 9233	2,460 ± 110	2,250–2,640
Wallaby 24	ANU 9234	3,350 ± 80	3,180–3,460
Wallaby 31	ANU 9236	4,140 ± 90	3,950–4,270
PCB 1	ANU 8896, 8897	70 ± 70	0–280
PCB 2	ANU 9037, 8901, 8898	300 ± 45	290–480
PCB 3	ANU 8899, 8902–8905	465 ± 30	480–545
PCB 4	ANU 8907–8909, 8911	565 ± 30	520–650
PCB 5	ANU 8914, 8915	785 ± 50	660–910
PCB 6	ANU 8916–8919, 8923	1,060 ± 35	930–1,060
PCB 7	ANU 8922, 8924, 8925	1,190 ± 35	1,000–1,270
PCB 8	ANU 8926–8930, 8932	1,360 ± 30	1,230–1,340
PCB 9	ANU 8934, 8936, 8937	1,730 ± 30	1,550–1,720
PCB 10	ANU 8938–8940	1,930 ± 60	1,720–1,960
PCB 11	ANU 8942–8945	1,965 ± 40	1,840–2,050
PCB 12	ANU 8946–8950, 8941	2,525 ± 50	2,350–2,760
Red Cliff 4	Wk 9613–9616	400 ± 50	0–170
Fitzroy 1	Wk 7979, 7980	Modern	
Fitzroy 2	Wk 7983, 7984	380 ± 50	0–148
Normanby 1	Wk 8019, 8017	Modern	
Normanby 2	Wk 8016, 8018	380 ± 50	0–148
Curacoa 1	ANU 8477, 9932, 9936	35 ± 35	30–260
Curacoa 2	ANU 9931, 9933, 9934	85 ± 40	20–270
Curacoa 3	ANU 9897	120 ± 80	10–310
Curacoa 4	ANU 8479, 8480, 9935	530 ± 50	500–650
Curacoa 5	ANU 8482–8486	1,010 ± 50	790–1,050
Curacoa 6	ANU 8487, 8488	1,100 ± 50	930–1,150
Curacoa 7	ANU 8490–8492, 9991	1,475 ± 32	1,310–1,480
Curacoa 8	ANU 8493–8495, 8497	1,675 ± 45	1,480–1,700
Curacoa 9	ANU 8505, 9984, 9987	2,065 ± 40	1,930–2,150
Curacoa 10	ANU 8519–8521, 8498	2,240 ± 30	2,150–2,340
Curacoa 11	ANU 9989, 9992	2,540 ± 50	2,410–2,760
Curacoa 12	ANU 8504, 8517, 8518	2,830 ± 40	2,850–3,070
Curacoa 13	ANU 8501, 9994	3,025 ± 55	3,050–3,360
Curacoa 14	ANU 8502, 8506, 8507	3,360 ± 40	3,480–3,710
Curacoa 15	ANU 8516, 9997	3,640 ± 50	3,840–4,130
Curacoa 16	ANU 8514, 9996	3,780 ± 55	3,990–4,400
Curacoa 17	ANU 8547–8549	4,070 ± 75	4,410–4,820
Curacoa 18	ANU 8508, 9998	4,230 ± 55	4,580–4,960
Curacoa 19	ANU 8510, 9999	4,410 ± 55	4,870–5,270
Curacoa 20	ANU 8511, 10000	4,820 ± 55	5,340–5,720
Curacoa 21	ANU 8512	5,095 ± 80	5,660–6,090
Curacoa 22	ANU 8513, 10001	5,620 ± 60	6,310–6,610

Note progressive increase in age for each ridge/storm deposit inland. Ridge 1 at each location is the seaward ridge. All values in the radiocarbon age column are group mean reservoir-corrected ages, except for Wk ages which are group mean conventional ages.

been less intense (929–931 hPa) than elsewhere; however, the lower elevation of these ridges may be due to limited sediment supply<sup>22</sup> rather than less intense cyclones.

The frequency of category 5 cyclones in the GBR region has previously been assumed to be once every several millennia<sup>7,12–14</sup>.

**Table 2 Central pressure of tropical cyclones responsible for emplacing ridges and eroding terraces**

Location	Inun. (m)	H <sub>s</sub> (m)	Set-up (m)	Run-up (m)	Surge (m)	Mean central pressure (hPa)	±1σ	±2σ
Wallaby	5.08	3.9	0.39	1.2	3.43	861	9	30
Wallaby	4.1	3.6	0.36	1.1	2.58	896	8	29
Wallaby	3.6	3.4	0.38	1.0	2.24	910	8	29
PCB	3.1	2.32	0.23	0.7	2.17	924	9	30
PCB	2.9	2.26	0.22	0.67	1.99	931	9	29
Red Cliff	6.1	5.2	0.52	1.56	3.99	900	12	25
Red Cliff	4.9	4.7	0.47	1.4	3.0	926	12	24
Red Cliff	3.8	4.13	0.41	1.24	2.11	949	12	23
Red Cliff	2.12	3.1	0.31	0.92	0.86	982	10	17
Fitzroy	4.5	7.4	0.74	2.2	1.5	894	20	39
Fitzroy	3.9	6.7	0.67	2.0	1.2	912	19	36
Normanby	4.71	7.9	0.79	2.4	1.4	893	13	31
Normanby	3.8	6.7	0.67	2.0	1.0	924	12	29
Curacoa	5.5	6.3	0.63	1.89	2.95	893	9	29
Curacoa	4.8	5.8	0.58	1.73	2.47	912	8	28
Lady	5.1	11.2	1.12	3.4	0.52	896	15	35
Lady	4.9	10.6	1.06	3.2	0.47	906	14	32
Lady	4.5	9.9	0.99	3.0	0.43	916	14	30

'Lady', Lady Elliot Island; Inun., inundation or height of ridge or terrace; H<sub>s</sub>, significant wave height. Lower inundation heights represent heights of lower storm deposits/ridges and terraces. Mean central pressure represents cyclone intensity if storm crossed at mean tide level, which is the dominant tide level over the full nodal (~19-yr) tidal cycle. Central pressures are regarded as minimum intensity values (see Methods).

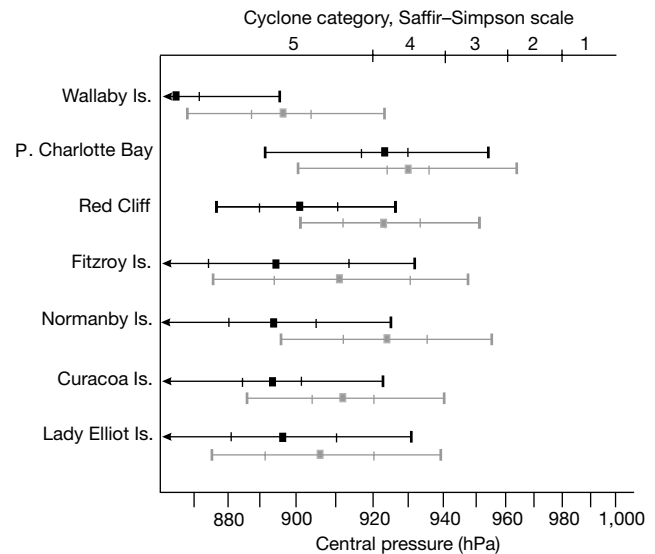


**Figure 2** Central pressures (mean, 1σ, 2σ) of cyclones responsible for building ridges and eroding terraces at study sites. Black lines represent cyclone intensities responsible for the emplacement of most ridges at sites. Grey lines indicate less-intense cyclones responsible for constructing and eroding lower-elevation ridges and terraces, respectively. Central pressures reported here must be regarded as minimum intensity values, as ridge heights represent the minimum elevation of storm inundation (see Methods).

Our results suggest that these events occur every 200–300 yr within all regions of the GBR between latitudes 13° and 24° S, and also within the Gulf of Carpentaria. We believe that our sites are representative of the long-term frequency of extreme intensity cyclones as they occur across a wide variety of environments along virtually the entire GBR. Our modelling results also agree closely with the levels of inundation and central pressures recorded during historical cyclones at Red Cliff (category 2 events in 1997 and 2000), Curacoa (category 3 event in 1971) and near PCB (category 5 event in 1899).

Extreme-intensity cyclones can cause destruction of substantial areas of rainforest and coral reefs. Large-scale severe wind disturbances elsewhere have resulted in forest gaps thousands of hectares in area, with up to 87–100% tree mortality with subsequent recruitment and succession<sup>18,23</sup>. More severe storms, such as the super-cyclones occurring every two to three centuries in northeast

Australia, would likewise result in large areas of tree mortality, uprooting and eventual succession.

The damage incurred by coral communities from severe intensity cyclones can also be devastating<sup>5</sup>. There is substantial spatial variation in damage following cyclones<sup>1,5,24,25</sup>, and storms of different intensity can have varied effects<sup>5</sup>. However, even in rare cases where extreme cyclones do not cause extensive damage to coral communities, they weaken the substrate, allowing severe damage to occur during subsequent less intense events<sup>25</sup>. Hence the frequency of the most intense cyclones is critical to the level of damage experienced by these communities over the longer term. The frequency of these extreme events may also place constraints upon the longevity of individual corals. Whereas some corals live up to 700 yr, most corals on the GBR rarely live beyond a few centuries<sup>26</sup>. Only the highest storm waves are capable of dislodging the largest of these long-lived corals, and such extreme conditions are likely to occur only during super-cyclones. That these events occur at time intervals less than the life span of many individual corals and trees suggests that the character of these communities must be strongly influenced by these high-magnitude storms.

The inferred frequency of super-cyclones is sufficiently high to have serious implications for the vulnerability of coastal human settlements. The twentieth century in northeast Australia was devoid of any category 5 cyclones, with only one such event (1899) since European settlement in the mid nineteenth century. The GBR region, however, experienced at least five such storms over the past 200 yr, with the area now occupied by Cairns experiencing two super-cyclones between 1800 and 1870 (Table 1). The periodicity of these storms suggests that community vulnerability, exposure and risk is much higher than previously estimated.

Short-term historical records in this region, and probably elsewhere throughout the global tropics, are inadequate for determining future effects of tropical cyclones on human society and their role as disturbance mechanisms upon ecological communities. Assessing these effects requires decoupling the role of human-induced climate change from natural quasi-periodicities, and this can only be achieved through the examination of longer-term records. □

## Methods

Surge heights were modelled using GCO2MD<sup>27</sup>—a numerical model that solves a set of mathematical equations over an equally spaced grid to determine water depth, currents, topography and bathymetry, and incorporates wind stresses and atmospheric pressure gradients acting on the ocean surface, and friction on the ocean floor. These results were compared with the maximum envelope of oceanic waters (MEOW) model<sup>28</sup> and with an empirical model—the Jelesnianski–Trajer nomogram technique<sup>29</sup>: these three models produced similar results. The relationship between surge height and angle of cyclone approach, cyclone translational velocity, radius of maximum winds ( $R_m$ ) and central pressure was determined for each site. Surge was found to increase with increases in each of these factors, but because their respective magnitudes are unknown for the palaeo-event, their mean probability magnitude level was calculated from the historical record of tropical cyclones in the region. The mean translational velocity of cyclones in this region is  $15.5 \pm 6.6 \text{ km h}^{-1}$ ,  $R_m$  is  $30 \pm 10 \text{ km}$ , and cyclone approach angle is  $63.8^\circ \pm 27.1^\circ$  (ref. 14). We used the 99% probability level of occurrence for the velocity and  $R_m$  (translational velocity  $40 \text{ km h}^{-1}$ ,  $R_m = 60 \text{ km}$ ), and an approach angle of  $37^\circ$  (being the angle producing the highest possible surge) for all of our surge model analyses. All modelled cyclones crossed the coast with the zone of greatest wind velocity occurring generally less than 5 km from each of the shingle ridge or terrace study sites.

Wave characteristics were determined using a nearshore shallow water wave model incorporating the GBR and local bathymetry and run in conjunction with the surge model. Wave set-up was estimated at 10% of significant wave height ( $H_s$ ), and run-up determined at 30% of  $H_s$ , on the basis of observations of run-up during three cyclone events in March 1997, February 1999 and February 2000 at Red Cliff and Fitzroy island. These observations involved the recording of total inundation by pre-placed markers at the sites, both the modelled and direct tide gauge measurements of the surge height, calculation of the wave set-up at 10% of  $H_s$  and direct measurement of  $H_s$  by an offshore wave-rider buoy in water of depth 15–20 m. The mean central pressure of the cyclone was determined as follows: the central cyclone pressure that produces 30% of  $H_s$  (measured run-up) and 10% of  $H_s$  (calculated wave set-up) is equal to the central cyclone pressure that produces the necessary surge height; the sum of these three components of the water column (run-up, set-up and surge) plus the tide level is equivalent to the height of the terrace or shingle ridge. Uncertainty margins reflect possible  $1\sigma$  and  $2\sigma$  tide range, determined from frequency distribution nodal tide curve for each site.

Cyclone frequency for PCB, Curacao, Lady Elliot and Wallaby islands was calculated from the average interval in years between ridge-building or storm-deposit events from the youngest to the oldest ridges dated from <sup>14</sup>C determinations. A total of 40 dates from 9 ridges at Lady Elliot island, 68 dates from 16 ridges at Curacao island and 65 dates from 12 ridges at PCB show no change in frequency in ridge-building events over the past several millennia, and a progressive increase in age of each ridge inland<sup>8–11</sup> (Fig. 1b). Ascertaining the most recent inundations of the ridges at Fitzroy and Normanby islands required collection of coral fragments from ridge crests. Although both sites returned recent ages (after AD 1800, it is highly unlikely that ridges at each site were deposited during the same event as coral fragments from the landward ridge were covered in lichen (shading by trees and so on has not influenced lichen growth) and had a more weathered appearance. The landward ridge is therefore interpreted as an older (and separate) storm deposit than its seaward counterpart. Grain size analyses of the gravels comprising the terraces at Red Cliff show they are well sorted, and (apart from the lower terrace) show no sign of grain size variations from the toe to the crest of each terrace. This indicates that the upper three terraces are erosional features, and that the deposit is a single depositional unit. As coral fragments younger than AD 1800 are buried in the top terrace, it can be assumed each of the lower terraces are younger again. Ridge heights represent the minimum level of inundation during a cyclone event, and therefore our estimates of palaeo-cyclone intensity must be regarded as minima. Indeed, morphological and sedimentological evidence at the multiple ridge sites suggest that these ridge sequences have been compacted over time and regularly over-topped by storm inundation since deposition, effectively reducing the original ridge height.

Received 20 February; accepted 21 August 2001.

- Connell, J. Diversity in tropical rainforests and coral reefs. *Science* **199**, 1302–1310 (1978).
- Sousa, W. The role of disturbance in natural communities. *Annu. Rev. Ecol. Syst.* **15**, 353–391 (1984).
- Tanner, J. *et al.* The role of history in community dynamics: A modelling approach. *Ecology* **77**, 108–117 (1996).
- Hughes, T. & Connell, J. Multiple stressors on coral reefs: A long-term perspective. *Limnol. Oceanogr.* **44**, 932–940 (1999).
- Connell, J. *et al.* A 30 year study of coral abundance, recruitment and disturbance at several scales in space and time. *Ecol. Monogr.* **67**, 461–488 (1997).
- Oliver, J. & Britton, N. *Natural Hazards and Reinsurance* (Cumberland College Health Sciences, Sydney, Australia, 1989).
- Walsh, K. *et al.* *Climate Change in Queensland under Enhanced Greenhouse Conditions* (Third annual report 1999–2000, CSIRO Atmospheric Research, Aspendale, Victoria, Australia, 2001).
- Chappell, J. *et al.* Holocene palaeo-environmental changes, central to north Great Barrier Reef inner zone. *BMR J. Aust. Geol. Geophys.* **8**, 223–235 (1983).
- Chivas, A. *et al.* Radiocarbon evidence for the timing and rate of island development, beach rock formation and phosphatization at Lady Elliot Island, Queensland, Australia. *Mar. Geol.* **69**, 273–287 (1986).
- Hayne, M. & Chappell, J. Cyclone frequency during the last 5,000 yrs from Curacao Island, Queensland. *Palaeoogeogr. Palaoclimatol. Palaeoecol.* **168**, 201–219 (2001).
- Hayne, M. & Chappell, J. A record of cyclone frequency from Princess Charlotte Bay, Nth Qld, Australia. *Palaeoogeogr. Palaoclimatol. Palaeoecol.* (in the press).
- Lourensz, H. Tropical cyclones in the Australian region, July 1909 to June 1980. (Bureau of Meteorology, Melbourne, 1981).
- Harper, B. *Storm Tide Threat in Queensland: History, Prediction and Relative Risks* (Technical report 10, Queensland Department of Environment & Heritage, Brisbane, 1998).
- McInnes, K. *et al.* *Cyclones Impacts on Tourism, Cairns, Nth Queensland* (CSIRO Report, CSIRO Tourism, Melbourne, 2000).
- Hubbell, S. *et al.* Light gap disturbances, recruitment limitation, and tree diversity in a neotropical rainforest. *Science* **283**, 554–557 (1999).
- Bryant, E. *Natural Hazards* (Cambridge Univ. Press, Cambridge, 1991).
- Henderson-Sellers, A. *et al.* Tropical cyclones and global climate change; a post IPCC assessment. *Bull. Am. Meteorol. Soc.* **79**, 19–38 (1998).
- Blumenstock, D. Typhoon effects at Jaluit Atoll in the Marshall Islands. *Nature* **182**, 1267–1269 (1958).
- Maragos, J. *et al.* Tropical cyclone creates a new land formation on Funafuti Atoll. *Science* **181**, 1161–1164 (1973).
- Fitchett, K. Physical effects of Hurricane Bebe upon Funafete Atoll, Tuvalu. *Aust. Geographer* **18**, 1–7 (1987).
- Scoffin, T. The geological effects of hurricanes on coral reefs and the interpretation of storm deposits. *Coral Reefs* **12**, 203–221 (1993).
- Chappell, J. & Grindrod, J. in *Coastal Geomorphology in Australia* (ed. Thom, B.) 197–231 (Academic, Sydney, 1984).
- Everham, E. & Brokaw, N. Forest damage and recovery from catastrophic wind. *Bot. Rev.* **62**, 113–184 (1996).
- Hughes, T. Community structure and diversity of coral reefs: The role of history. *Ecology* **7**, 275–279 (1989).
- Lirman, D. & Fong, P. Susceptibility of coral communities to storm intensity, duration and frequency. *Proc. 8th Int. Coral Reef Symp.* (eds Lessios, H. & MacIntire, I.) Vol. 1, 561–566 (Smithsonian Tropical Research Institute Balboa, Panama, 1997).
- Potts, D. C. *et al.* Dominance of a coral community by the genus *Porites*. *Mar. Ecol. Prog. Ser.* **23**, 79–84 (1985).
- Hubbert, G. & McInnes, K. A storm surge inundation model for coastal planning and impact studies. *J. Coast. Res.* **15**, 168–185 (1999).
- Sanderson, B. *et al.* *A Tropical Cyclone Maximum Envelope of Waters (MEOW) Technique* (Applied Mathematics Report 95/28, Department of Mathematics, Monash Univ. Clayton, Victoria, Australia, 1995).
- US Army Corps of Engineers *Shore Protection Manual* (US Army Coastal Engineering Research Centre, Washington, 1986).

## Acknowledgements

We thank J. Wright, J. Tanner and H. Marsh for comments on the manuscript; T. Hughes, J. Chappell, G. Hubbert and S. Oliver for discussions on the topic; and J. H. Choat and R. Pearson for early encouragement of this project. M.H. publishes with the permission of the Chief Executive Officer of AGSO.

Correspondence and requests for material should be addressed to J.N. (e-mail: Jonathan.Nott@jcu.edu.au).

## Multiple benefits of gregariousness cover detectability costs in aposematic aggregations

Marianna Riipi\*, Rauno V. Alatalo, Leena Lindström & Johanna Mappes

University of Jyväskylä, Department of Biological and Environmental Science, Konnevesi Research Station, PO Box 35, FIN-40 351 Jyväskylä, Finland

Understanding the early evolution of aposematic (warning) coloration has been a challenge for scientists, as a new conspicuous morph in a population of cryptic insects would have a high predation risk and would probably die out before local predators learnt to avoid it<sup>1–4</sup>. Fisher<sup>5</sup> presented the idea of aggregation benefit through the survival of related individuals; however, his theory has been strongly debated<sup>6–8</sup> as the mechanisms that favour grouping have never been explored experimentally with the incorporation of detectability costs. Here we create a comprehensive ‘novel world’ experiment with the great tit (*Parus major*) as a predator to explore simultaneously the predation-related benefits and costs for aposematic aggregated prey, manipulating both group size and signal strength. Our results show that grouping would have been highly beneficial for the first aposematic prey individuals surrounded by naive predators, because (1) detectability risk increased only asymptotically with group size; (2) additional detectability costs due to conspicuous signals were marginal in groups; (3) even naive predators deserted the group after detecting unpalatability (dilution effect); and (4) avoidance learning of signal was faster in groups. None of these mechanisms require kin selection.

In the first experiment we tested how signal strength and group size affects the risk of prey detection. We used the ‘novel world’ method<sup>6,9</sup> because it uses a fundamental property of warning signals, conspicuousness, but presents the predators with signals not found in their natural environment. As prey, we used pieces of almond glued between two pieces of paper that had the signal printed on them. The birds were simultaneously presented with nine different palatable prey assemblages—combinations of three group sizes (1, 4 or 8 prey items) and three signals (a cross symbol with a square set at the centre: the size of the square varied according to the signal number, that is, small (signal 2) to large (signal 4); see Fig. 1). The background on the aviary floor consisted of white paper sheets with the cryptic signal (signal 1: a cross symbol without a square) printed on them. Each prey assemblage was presented four times in random locations on the background. Increasing group size caused an increase in the number of those assemblages that were attacked by the birds ( $F = 84.32$ , degrees of freedom (d.f.) = 2;  $P < 0.001$ ), owing to an increase in prey detectability. Prey groups had higher detectability risk than solitary prey, but this risk did not increase in direct proportion to group size (this effect is sometimes called concealment<sup>10</sup> or avoidance effect<sup>11</sup>) (Fig. 2).

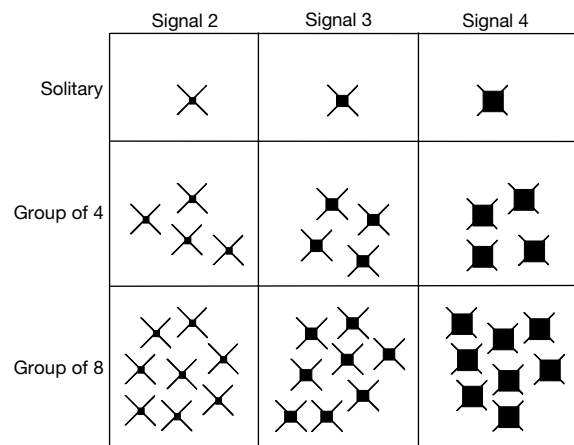


**Figure 1** Prey assemblages used in the detectability experiment. Each assemblage was presented in the aviary in four replicates, and thus there were 36 assemblages in total.

Increasing signal strength caused an increase in the number of those assemblages that were attacked by the birds ( $F = 9.91$ , d.f. = 2,  $P < 0.001$ ). For solitary prey, a strong signal (signal 4) increased the detectability of the prey twofold (100%) compared with signal 2 (Fig. 2;  $t$ -test between solitary signal 2 and 4,  $t = 3.80$ , d.f. = 64,  $P = 0.001$  after Bonferroni correction), whereas in groups of four or eight prey items the increase in the detectability of the group caused by the strong signal was only 12.5% and 13.3%, respectively (Fig. 2; group of 4:  $t = 1.34$ , d.f. = 64,  $P = 0.561$ ; group of 8:  $t = 1.69$ , d.f. = 64,  $P = 0.288$  after Bonferroni correction). Thus, signal strength caused little additional increase in detectability when in a group, suggesting that the cost of a strong signal could be smaller for aggregations than for solitary prey. Previously, the effect of the strength of an aposematic signal on the detectability of prey has been assumed to be similar for both a small group (under 20 individuals) and for solitary prey<sup>10,12</sup>.

If the increased detectability of a group compared with solitary prey does not translate into increased mortality risk per individual, then grouping is always more favourable than a solitary lifestyle. A decreased per capita mortality risk can be produced by a dilution effect, which means that when a predator cannot eat the whole group, an individual's chance of being eaten is smaller in a group than when it is solitary<sup>10,11,13</sup>. To show the effect of dilution, we used the detectability data (Fig. 2) to calculate estimates of relative mortality for average prey individuals in different group sizes in situations where the predator tastes a certain number of prey items from a group (Table 1). This simulates different levels of predator satiation<sup>12</sup>, for example, if the prey is very unpalatable the predator may leave the group after tasting only one individual. Naturally, the real group sizes favoured by selection are dependent on the predator and prey in question, but the general idea is that prey individuals with strong signals benefit most from gregariousness, because their detectability is increased only slightly by grouping (Table 1).

In the second experiment, we performed learning tests with six groups of birds in a factorial design with two signal levels (signal 2 (weak) and signal 4 (strong)) and three prey group sizes. Each bird was presented with solitary, palatable cryptic items (the symbol on the prey was similar to the background symbol) together with unpalatable prey items carrying a signal of only one type. Solitary cryptic prey were palatable to mimic a situation where a distasteful aposematic morph evolves in an environment where most of the cryptic species are palatable; there is thus a reward of learning to avoid the aposematic prey. The tests were carried out in five consecutive days for each bird, and numbers of cryptic and aposematic prey eaten at the trials were recorded. Survival of unpalatable prey with the weak signal (signal 2) increased with group size (Fig. 3a;  $F_{(2,20)} = 3.74$ ,  $P = 0.042$ ). The birds did not learn to avoid

\* Present address: Section of Ecology, Department of Biology, University of Turku, FIN-20014 Turku, Finland.